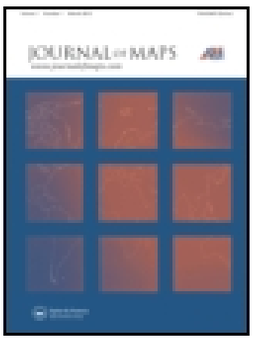

Taylor & Francis
Taylor & Francis Group

Journal of Maps

ISSN: (Print) 1744-5647 (Online) Journal homepage: https://www.tandfonline.com/loi/tjom20

Morphological and geological features of Drake Passage, Antarctica, from a new digital bathymetric model

F. Bohoyo, R. D. Larter, J. Galindo-Zaldívar, P. T. Leat, A. Maldonado, A. J. Tate, M. M. Flexas, E. J. M. Gowland, J. E. Arndt, B. Dorschel, Y. D. Kim, J. K. Hong, J. López-Martínez, A. Maestro, O. Bermúdez, F. O. Nitsche, R. A. Livermore & T. R. Riley

To cite this article: F. Bohoyo, R. D. Larter, J. Galindo-Zaldívar, P. T. Leat, A. Maldonado, A. J. Tate, M. M. Flexas, E. J. M. Gowland, J. E. Arndt, B. Dorschel, Y. D. Kim, J. K. Hong, J. López-Martínez, A. Maestro, O. Bermúdez, F. O. Nitsche, R. A. Livermore & T. R. Riley (2019): Morphological and geological features of Drake Passage, Antarctica, from a new digital bathymetric model, Journal of Maps, DOI: 10.1080/17445647.2018.1543618

To link to this article: https://doi.org/10.1080/17445647.2018.1543618

JOURNAL OF MAPS
https://doi.org/10.1080/17445647.2018.1543618

Taylor & Francis
Taylor & Francis Group

Science

OPEN ACCESS Check for updates

Morphological and geological features of Drake Passage, Antarctica, from a new digital bathymetric model

F. Bohoyo [a], R. D. Larter [b], J. Galindo-Zaldívar[c,d], P. T. Leat[b], A. Maldonado[d], A. J. Tate [b], M. M. Flexas[e], E. J. M. Gowland[b], J. E. Arndt [f], B. Dorschel[f], Y. D. Kim[g], J. K. Hong[g], J. López-Martínez[h], A. Maestro [a,h], O. Bermúdez[a], F. O. Nitsche[i], R. A. Livermore[j] and T. R. Riley [b]

[a]Instituto Geológico y Minero de España, Madrid, Spain; [b]British Antarctic Survey, Cambridge, UK; [c]Departamento de Geodinámica, Universidad de Granada Granada, Spain; [d]Instituto Andaluz de Ciencias de la Tierra (IACT), Granada, Spain; [e]Jet Propulsion Laboratory, Pasadena, CA, USA; [f]Alfred Wegener Institute, Bremerhaven, Germany; [g]Korea Polar Research Institute, Incheon, Korea; [h]Departamento de Geología y Geoquímica, Universidad Autónoma de Madrid, Madrid, Spain; [i]Lamont-Doherty Earth Observatory, Columbia University, Palisades, NY, USA; [j]The Open University, Milton Keynes, UK

ABSTRACT

The Drake Passage is an oceanic gateway of about 850 km width located between South America and the Antarctic Peninsula that connects the southeastern Pacific Ocean with the southwestern Atlantic Ocean. It is an important gateway for mantle flow, oceanographic water masses, and migrations of biota. This sector developed within the framework of the geodynamic evolution of the Scotia Arc, including continental fragmentation processes and oceanic crust creation, since the oblique divergence of the South American plate to the north and the Antarctic plate to the south started in the Eocene. As a consequence of its complex tectonic evolution and subsequent submarine processes, as sedimentary infill and erosion mainly controlled by bottom currents and active tectonics, this region shows a varied physiography. We present a detailed map of the bathymetry and geological setting of the Drake Passage that is mainly founded on a new compilation of precise multibeam bathymetric data obtained on 120 cruises between 1992 and 2015, resulting in a new Digital Bathymetric Model with 200 × 200 m cell spacing. The map covers an area of 1,465,000 km^2 between parallels 52°S and 63°S and meridians 70°W and 50°W at scale 1:1,600,000 allowing the identification of the main seafloor features. In addition, the map includes useful geological information related to magnetism, seismicity and tectonics. This work constitutes an international cooperative effort and is part of the International Bathymetric Chart of the Southern Ocean project, under the Scientific Committee on Antarctic Research umbrella.

ARTICLE HISTORY
Received 16 May 2018
Accepted 30 October 2018

KEYWORDS
Bathymetry; seafloor; Drake Passage; Scotia-Arc; Antarctica

1. Introduction

The opening of the main Southern Ocean gateways, Drake Passage and the Tasmanian gateway separating South America and Australia from Antarctica respectively, enabled the present-day global ocean circulation pattern to develop (Kennett, 1977; Lawver, Gahagan, & Dalziel, 2011; Livermore, Nankivell, Eagles, & Morris, 2005, Livermore, Hillenbrand, Meredith, & Eagles, 2007; Maldonado et al., 2014; Scher & Martin, 2006; Scher et al., 2015). This allowed extensive exchange of water between the main ocean basins and led to the development of the Antarctic Circumpolar Current (ACC), which contributed to the thermal isolation of Antarctica, and was partially responsible for global cooling at the Eocene-Oligocene boundary and played an important role in late Miocene cooling (Barker, 2001; Eagles & Jokat, 2014; Kennett, 1977; Lawver & Gahagan, 2003; Martos, Galindo-Zaldívar, Catalán, Bohoyo, & Maldonado, 2014; Naveira-Garabato, Heywood, & Stevens, 2002; Pearce, Leat, Barker, & Millar, 2001; Roterman, Copley, Linse, Tyler, & Rogers, 2013).

The Drake Passage is an oceanic gateway of about 850 km width located between South America and the Antarctic Peninsula that connects the southeastern Pacific Ocean with the southwestern Atlantic Ocean and influences exchanges of mantle flow, oceanographic water masses, and migrations of biota (Naveira-Garabato et al., 2002; Pearce et al., 2001; Roterman et al., 2013; Sievers & Nowlin, 1984). This gateway developed within the framework of the geological evolution of the Scotia Arc (Figure 1).

The map Bathymetry and Geological Setting of the Drake Passage was published originally by BAS and IGME, as paper copies, with support from SCAR, as the seventh sheet of the BAS GEOMAP 2 series at 1:1,500,000 scale (Bohoyo et al., 2016). We present here a new Digital Bathymetric Model (DBM), of the Drake Passage, named DBM-BATDRAKE, an improved version of the map of the Drake Passage, at 1:1,600,000 scale, and the description of how the map

CONTACT F. Bohoyo f.bohoyo@igme.es Instituto Geológico y Minero de España, Ríos Rosas, 23. 28003 Madrid, Spain

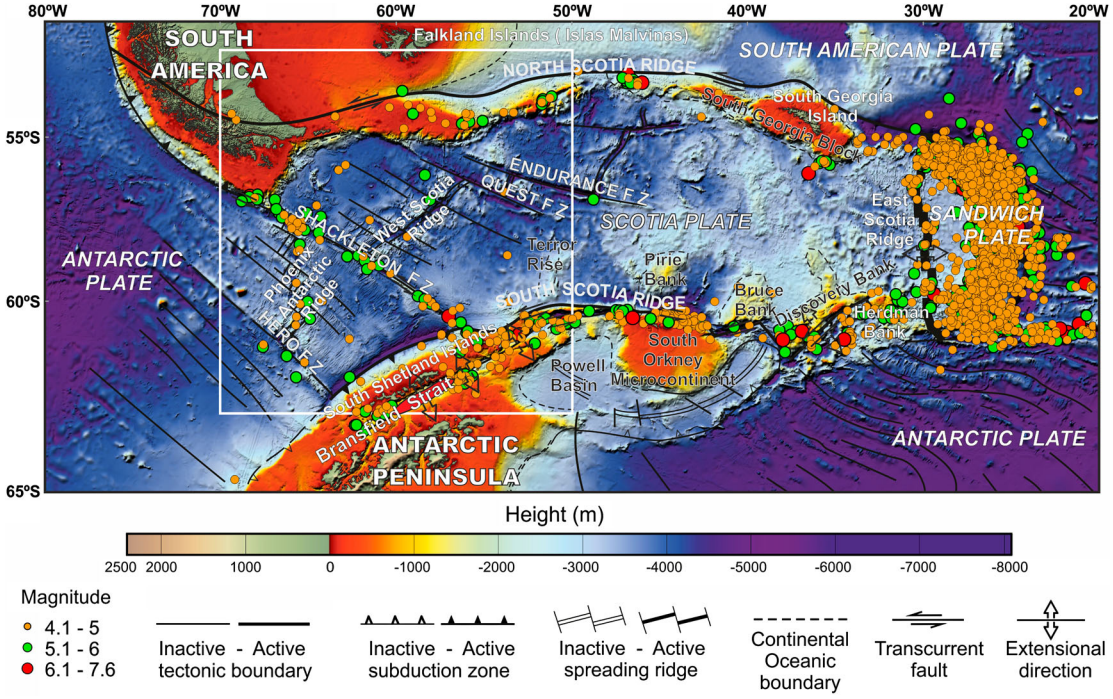

Figure 1. Geological map of the Scotia Arc. Bathymetry from GEBCO_2014 including IBCSO v1.0 below 60° S. White square identifies the study region.

complied with the bathymetry acquisition and geological regional context details.

The basis for the map and DBM are mainly founded on a compilation of precise multibeam bathymetric data obtained on 120 cruises between 1992 and 2015. DBM-BATDRAKE is gridded at 200 × 200 m spacing and covers an area of 1,465,000 km^2 between parallels 52°S and 63°S and meridians 70°W and 50°W. The map presents the new DBM at a scale of 1:1,600,000 that permits identification of the main seafloor features and their geographical relationships, and it includes additional useful geological information.

This first version of the multibeam data compilation, resulting in the DBM-BATDRAKE, constitutes an international cooperative effort coordinated by the Geological Survey of Spain (IGME), the British Antarctic Survey (BAS), the Alfred Wegener Institute (AWI) and the Korean Polar Research Institute (KOPRI), together with USA data available from the Lamont-Doherty Earth Observatory (LDEO). This initiative is part of the International Bathymetric Chart of the Southern Ocean (IBCSO) mapping project (Arndt et al., 2013), under the Scientific Committee on Antarctic Research (SCAR) umbrella, which recognizes the importance of regional data compilations and mapping programmes in areas of particular scientific interest around Antarctica, such as the Ross Sea, Drake Passage and the southern margin of the Weddell Sea.

1.1. Geological Setting

The development of the Scotia Sea, that contains several active and extinct spreading ridges, is directly related to the opening of Drake Passage, which results from fragmentation of the continental connection between South America and the Antarctic Peninsula during the final steps of Gondwana breakup, followed by onset of seafloor spreading in the southwestern part of the Scotia Sea during late Eocene and the initiation of the West Scotia Ridge (WSR) during the Oligocene (Barker & Burrell, 1977; Eagles, Livermore, Fairhead, & Morris, 2005). The Scotia Arc includes the Scotia and Sandwich plates, and is bounded to the north by the North Scotia Ridge, to the south by the South Scotia Ridge, to the west by the Shackleton Fracture Zone, and to the east by the South Sandwich Trench (Figure 1). Continental fragments as submerged banks and volcanic edifices form the Scotia Arc relieves around the deep basins of the Scotia Sea (Figure 1; Barker, 2001; Barker, Dalziel, & Storey, 1991; Eagles & Jokat, 2014; Lawver & Gahagan, 2003; Livermore, McAdoo, & Marks, 1994).

The Shackleton Fracture Zone (SFZ) occupies a central position in the Drake Passage and is an intra-oceanic ridge which rises several hundreds to thousands of metres above the surrounding seafloor. The SFZ separates the Scotia Plate of the Scotia Sea to the east and the Antarctic and former Phoenix plates to the west, which underlie the southeastern part of the Pacific Ocean. The SFZ is an active transpressional and left-lateral transcurrent fault that accommodates, in conjunction with the North Scotia Ridge and South Scotia Ridge, the relative motion between the Scotia Plate and the South-American and Antarctic plates and connects the Chile Trench with the South Shetland Trench (Smalley Jr. et al., 2007; Thomas, Livermore, & Pollitz, 2003). The SFZ is underthrusted below Elephant Island

(Aldaya & Maldonado, 1996; Galindo-Zaldívar et al., 2006). The SFZ intersects two extinct spreading centres – the West Scotia Ridge and the Phoenix–Antarctic Ridge – between which the SFZ acted as an oceanic ridge-to-ridge transform fault when both spreading centres were active (Livermore et al., 2000, 2004; Maldonado et al., 2000). The geodynamic evolution of the region, seismic activity and tectonic data suggest a complex evolution of the Drake Passage such that the SFZ began as an oceanic transform fault with strike-slip motion along most of its length and later became a transpressive transcurrent fault zone as it remains today (Livermore, Eagles, Morris, & Maldonado, 2004). Uplift of the SFZ in the last 8 Ma has formed a barrier for oceanic bottom currents (Figure 1; Livermore et al., 2004).

Spreading at the Phoenix-Antarctic Ridge ended during chron C2A (2.6-3.6 Ma), when the Phoenix Plate became part of the Antarctic Plate, and following a long period of late Mesozoic and Cenozoic subduction of the Phoenix Plate below the Pacific Margin of the Antarctic Peninsula (Eagles, Gohl, & Larter, 2009; Larter & Barker, 1991; Livermore et al., 2000). Subduction continued at the South Shetland Trench due to rollback processes at the hinge of subduction and active spreading in the Bransfield Strait (González-Casado, Giner-Robles, & López-Martínez, 2000; Jabaloy et al., 2003; Larter & Barker, 1991; Maldonado, Larter, & Aldaya, 1994). The West Scotia Ridge formed most of the oceanic crust of the Scotia Sea from early Oligocene to its extinction after chron C3A (6.4 Ma) during a period of regional Scotia Sea compression after 17 Ma due to small change in the pole of rotation (Livermore et al., 2004). The West Scotia Ridge spreading segments are separated by former transform faults, among which the easternmost Endurance and Quest Fracture Zones are particularly prominent. Recent studies of the Drake Passage geodynamics suggest opening of oceanic basins that developed in the southwestern Scotia Arc during Eocene time (Figure 1; Eagles & Jokat, 2014; Maldonado et al., 2014).

The main geological structures and brittle deformation record in the western Scotia Arc reveal a complex geological history since the Mesozoic, which includes transform, convergent and divergent tectonic settings, and shows a regional NE-SW compression and a NW-SE extension regime at the present day (Bohoyo et al., 2007; Galindo-Zaldívar, Jabaloy, Maldonado, & Sanz de Galdeano, 1996; Maestro, López-Martínez, Galindo-Zaldívar, Bohoyo, & Mink, 2014).

2. Methods

2.1. Multibeam Data

Data from Multibeam echo sounders are the core of this compilation. Multibeam echo sounding systems send out an array of sound pulses in a fan shape, usually 90° to 150°, and returns depths from underneath the ship and from either side as well. This is sometimes referred to as a swath bathymetry as it produces a swath of depth information, the width of which is a simple function of the water depth and the coverage angle. As ships collecting multibeam data are constantly undergoing complex motion (rolling, pitching and yawing), this needs to be measured and corrections need to be applied to the transmitted beams. Surveys of the RRS James Clark Ross (United Kingdom), BIO Hespérides (Spain), RV Polarstern (Germany), RVIB Nathaniel B. Palmer (United States), and the RVs Araon and Onnuri (Korea) conducted between 1992 and 2015 generated all multibeam, from different acquisition swath systems, data used in DBM-BATDRAKE (Figure 2). The resulting database consisted of more than 83 million data points and approximately 65% of the offshore 200 × 200 m grid cells of DBM-BATDRAKE are constrained by sounding data.

In total, 120 multibeam cruises are included in the compilation (see Table 1). These range from large-scale systematic survey areas to data collection along single transit lines. The quality of the multibeam data sets varies substantially, depending on the acquisition date, multibeam system, and processing status.

Most of the data were obtained with Kongsberg EM12, 120 and 122 systems, which are installed at present in all of the vessels from which data were used except in RV Polarstern, which carries an Atlas Hydrosweep DS3 system. Sea Beam systems have been used too in the RVs Polarstern, NB Palmer and Onnuri in the 80's and 90's. Details about Kongsberg systems including number of beams, as well as typical coverage and swath width are synthetized in Table 2. Taking into account the properties of all of the systems, we chose 200 m cell resolution because it was the finest grid size that could be used consistently for data in the deepest areas collected with some of the earlier multibeam systems (e.g. the older Spanish cruises using EM12 up to 2004 with narrower coverage and fewer beams) without leaving a lot of empty cells.

The spatial distribution of the multibeam surveys is heterogeneous with a higher concentration in the central Drake region, around the Antarctic Peninsula and related with the ship transits from Port Stanley (Falkland Islands) and from the SE of South America (From Ushuaia, Argentina and Punta Arenas, Chile). Existing data coverage as at July of 2015 is shown in Figure 2, including both dedicated block-mapping of areas of particular interest such as Shackleton Fracture Zone, West Scotia Ridge, Phoenix-Antarctic Ridge, Bransfield Basin, and South Scotia Ridge among others and transit lines (Figures 1 and 2).

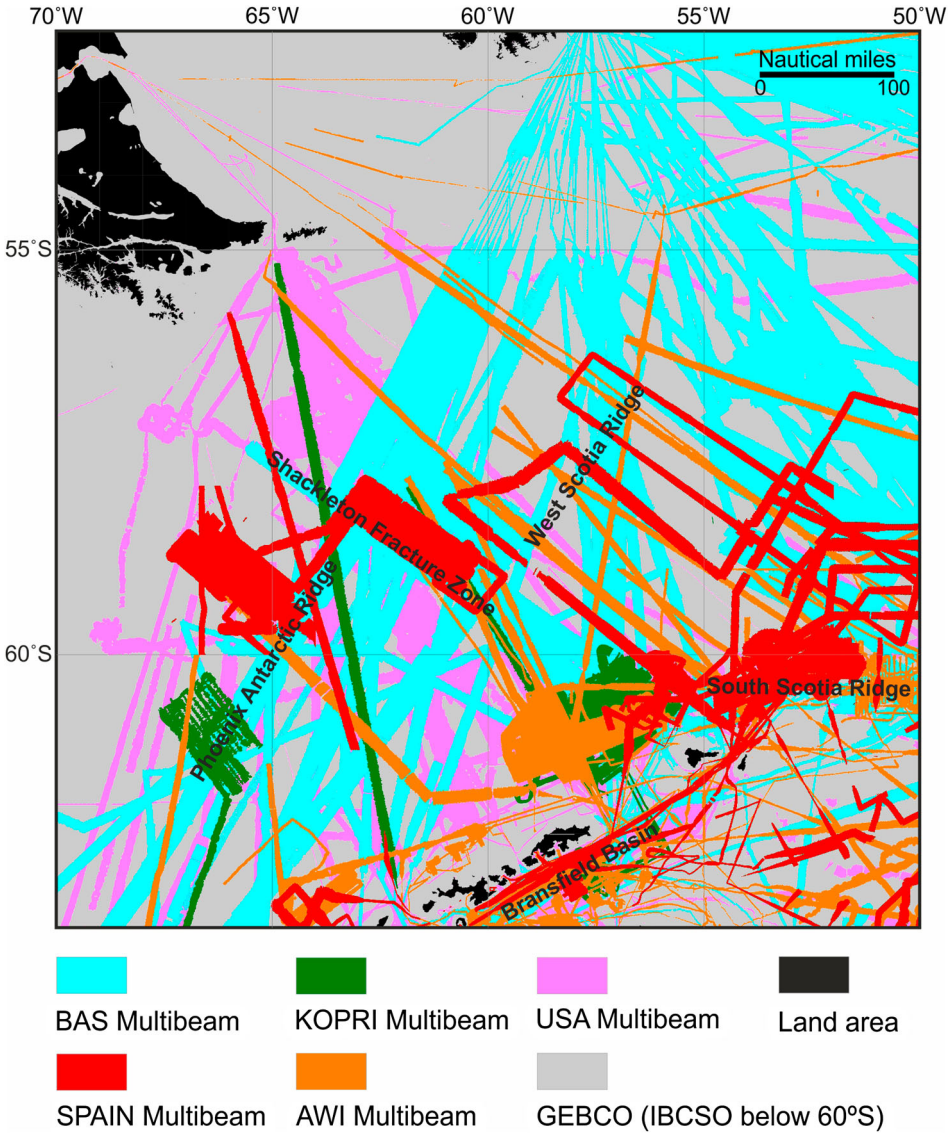

Figure 2. Map of bathymetry coverage compiled from a variety of different data sources (see Table 1).

2.2. Predicted Bathymetry

Despite the relatively dense multibeam data coverage, some data gaps up to 200 km in diameter exist. Most of these large gaps are located in the deep-sea areas of the Pacific Ocean in the western part of the map and in the shallow shelf waters of the Atlantic Ocean between South America and the Falkland Islands. These gaps were filled with data of the GEBCO_2014 grid (Weatherall et al., 2015) which south of 60°S consists of IBCSO version 1.0 (Arndt et al., 2013) at a different resolution. These data sets include singlebeam data sets and predicted bathymetry from gravity inversion of satellite radar altimetry (Figure 2). The predicted bathymetry derived from satellite altimetry is limited in resolution to 12–17 km (Becker et al., 2009) but it is capable of estimating seafloor topography even in areas that have not been directly surveyed by vessels (Schöne & Schenke, 1998). Hence, the resolution of the data used in the DBM-BATDRAKE data gaps can be more than 60 times lower than the 200 m resolution used for areas with multibeam bathymetry.

2.3. Digital Bathymetric Model BATDRAKE construction

The DBM-BATDRAKE was built adapting the workflow chart used in the IBCSO Version 1.0 (Arndt et al., 2013). The multibeam data from different sources, at least a large percentage of them, were edited to remove erroneous soundings and outlier points using dedicated software such as Neptune, Caris, MB-System and Fledermaus, and exported as ASCII XYZ datasets. The resulting data base with mostly processed and remaining unprocessed data, was then compiled using an iterative process consisting of gridding the sounding data stored, visualizing the result, identifying and cleaning spurious data points until satisfactory results were achieved. All data cleaning performed in this step was done directly on the ASCII XYZ data using QPS Fledermaus. For this, the ASCII XYZ data base was transferred to native QPS Fledermaus 'Pure File Magic' (.pfm) files that successively were cleaned in the 3D Editor, were then exported back to the ASCII XYZ format.

Table 1. Data sources order by institution, includes vessel, cruise name, year and multibeam system.

CRUISE	YEAR	SYSTEM	CRUISE	YEAR	SYSTEM	CRUISE	YEAR	SYSTEM
RV JAMES CLARK ROSS – British Antarctic Survey – BAS (United Kingdom)								
JR59	2001	EM120	JR114-121	2005	EM120	JR188	2009	EM120
JR60	2001	EM120	JR115	2004	EM120	JR193-196	2007	EM120
JR66	2001	EM120	JR116	2004	EM120	JR194-197	2008	EM120
JR69-67	2001	EM120	JR130	2004	EM120	JR206	2010	EM120
JR70	2002	EM120	JR130z	2004	EM120	JR224	2009	EM120
JR71	2002	EM120	JR134	2005	EM120	JR228	2009	EM120
JR72	2002	EM120	JR141	2006	EM120	JR230	2009	EM120
JR77-78	2004	EM120	JR149	2006	EM120	JR233	2009	EM120
JR81	2002	EM120	JR150	2006	EM120	JR239-235	2010	EM120
JR82	2003	EM120	JR151	2005	EM120	JR236	2010	EM120
JR84	2003	EM120	JR152-159	2006	EM120	JR240	2010	EM120
JR93	2003	EM120	JR157-166	2007	EM120	JR244	2011	EM120
JR93z	2003	EM120	JR158	2007	EM120	JR252-254C	2011	EM120
JR97	2005	EM120	JR165	2007	EM120	JR255A-B	2012	EM120
JR100	2004	EM120	JR168-167	2007	EM120	JR259	2012	EM120
JR103	2004	EM120	JR179	2008	EM120	JR275	2012	EM120
JR104	2004	EM120	JR184	2007	EM120	JR262-260A	2012	EM120
JR107	2004	EM120	JR185	2007	EM120	JR276	2011	EM120
JR109	2004	EM120	JR186	2008	EM120			
JR112	2005	EM120	JR187	2008	EM120			
CRUISE		YEAR	SYSTEM	CRUISE		YEAR	SYSTEM	
BIO HESPÉRIDES – Spanish Antarctic Programme (Spain)								
HESANT9293		1993	EM12	SCAN2008		2008	EM120	
SCAN97		1997	EM12	DRAKE2008		2008	EM120	
ANTPAC9798		1998	EM12	ELEFANTE2012		2012	EM120	
SCAN2001		2001	EM12	ELEFANTE2013		2013	EM120	
SCAN2004		2004	EM120	SCAN2013		2013	EM120	
CRUISE	YEAR	SYSTEM	CRUISE	YEAR	SYSTEM	CRUISE	YEAR	SYSTEM
RV POLARSTERN – Alfred Wegener Institute – AWI (Germany)								
ANT-IV/4	1986	Sea Beam	ANT-XV/4	1998	Hydrosweep DS-1	ANT-XXIII/4	2006	Hydrosweep DS-2
ANT-V/4	1987	Sea Beam	ANT-XVII/3	2000	Hydrosweep DS-2	ANT-XXIII/5	2006	Hydrosweep DS-2
ANT-VI/2	1987	Sea Beam	ANT-XVIII/4	2001	Hydrosweep DS-2	ANT-XXIII/7	2006	Hydrosweep DS-2
ANT-VI/3	1987	Sea Beam	ANT-XVIII/5	2001	Hydrosweep DS-2	ANT-XXIII/8	2006	Hydrosweep DS-2
ANT-VIII/4	1989	Sea Beam	ANT-XIX/4	2002	Hydrosweep DS-2	ANT-XXIII/9	2007	Hydrosweep DS-2
ANT-VIII/5	1989	Sea Beam	ANT-XIX/5	2002	Hydrosweep DS-2	ANT-XXVII/3	2011	Hydrosweep DS-2
ANT-IX/2	1990	Hydrosweep DS-1	ANT-XX/2	2002	Hydrosweep DS-2	ANT-XXIX/3	2013	Hydrosweep DS-2
ANT-XI/3	1994	Hydrosweep DS-1	ANT-XXII/2	2004	Hydrosweep DS-2	GAP95	1995	Hydrosweep DS-1
ANT-XII/3	1995	Hydrosweep DS-1	ANT-XXII/3	2005	Hydrosweep DS-2	GAP98	1998	Hydrosweep DS-1
ANT-XV/2	1997	Hydrosweep DS-1	ANT-XXII/4	2005	Hydrosweep DS-2			
CRUISE	YEAR	SYSTEM	CRUISE	YEAR	SYSTEM	CRUISE	YEAR	SYSTEM
RV NATHANIEL B PALMER – Unites States Antarctic Programme (United States of America)								
AMLR95	1995	Sea Beam 2112	NBP0002	2000	Sea Beam 2112	NBP0502	2005	EM120
NBP9507	1995	Sea Beam 2112	NBP0003	2000	Sea Beam 2112	NBP0506	2005	EM120
NBP9902	1999	Sea Beam 2112	NBP0103	2001	Sea Beam 2112	NBP0602A	2006	EM120
NBP9903	1999	Sea Beam 2112	NBP0104	2001	Sea Beam 2112	NBP0703	2007	EM120
NBP9904	1999	Sea Beam 2112	NBP0107	2001	Sea Beam 2112	NBP0805	2008	EM120
NBP9905	1999	Sea Beam 2112	NBP0201	2002	EM120			
NBP0001	2000	Sea Beam 2112	NBP0202	2002	EM120			
CRUISE	YEAR	SYSTEM	CRUISE	YEAR	SYSTEM	CRUISE	YEAR	SYSTEM
RV Onnuri- RV Araon (from 2010) – Korea Polar Research Institute - KOPRI (Germany)								
Korea93	1993	Sea Beam 2000	Korea99	1999	Sea Beam 2000	Korea2013	2013	EM120

The data have been gridded at two-resolutions to maintain a maximum of the seafloor morphology details where data density and quality are sufficient and, at the same time, to prevent the occurrence of artefacts in areas with sparse data. To do so, separate low- and high resolution grids were generated and merged those with a specific bending algorithm in a method similar to the remove-restore method used for IBCAO Version 3.0 and IBCSO Version 1.0 (Arndt et al., 2013; Hell & Jakobsson, 2011; Jakobsson et al., 2012; Smith & Sandwell, 1997).

In order to create the low-resolution 1000 × 1000 m grid, a weighted block median filter with the block size set to 2000 m was applied to the entire database using the GMT program "blockmedian". The blockmedian filtered points were subsequently gridded using the

Table 2. Acquisition resolution of SIMRAD systems.

SIMRAD		EM12	EM120	EM122
Beams		81	191	288
Coverage Angle		90°	120° (max 150°)	140° (max 150°)
Coverage		2*Depth	3.5*Depth	4.5*Depth (2–6)
Depth	Swath width	2000 m	3500 m	4500 m
1000 m	Cell resolution	~25 m	~20 m	~15 m
Depth	Swath width	6000 m	10,500 m	13,500 m
3000 m	Cell resolution	~75 m	~55 m	~47 m
Depth	Swath width	10,000 m	17500 m	22500 m
5000 m	Cell resolution	~125 m	~95 m	~79 m
Depth	Swath width	12,000 m	21000 m	27000 m (max)
6000 m	Cell resolution	~150 m	~110 m	~94 m

splines in tension algorithm included in the program "surface" of the Generic Mapping Tools (GMT) (Wessel & Smith, 1995) with a tension factor of 0.35. The resulting grid was then smoothed using a 2000 × 2000 m cosine filter of GMT's program "grdfilter" and subsequently resampled to 200 × 200 m resolution using GMT's "grdsample". The high-resolution 200 × 200 m grid was compiled only from spatially dense and high-quality data. We applied a weighted block median filter with the block size set to 200 m resolution on these data. These block median filtered points then were gridded using GMT's program "nearneighbor" at 200 × 200 m resolution. Using this approach, the high-resolution grid is limited to areas where high quality data exist. The high- and the low-resolution grid were combined in ArcGIS using the 'bending algorithm' described by Arndt et al. (2013) that minimizes the occurrence of edge effects caused by the different grid resolutions. The bending algorithm can be used universally for merging overlapping grids in conjunction with individually defined transition zones. For DBM-BATDRAKE we chose a transition zone of 400 m.

Finally, areas where no soundings constrained the gridding were filled with adjusted predicted bathymetry based on satellite altimetry from the GEBCO_2014 data set using the "gap-fill" method (Arndt et al., 2013). First, the GEBCO_2014 grid was adjusted to the soundings of the DBM-BATDRAKE database to minimize the difference to the interpolated grid derived only from soundings in the previous steps. For this, the vertical difference between sounding data and GEBCO_2014 was calculated using GMT's "grdtrack." On these difference points, a 10 km block median filter was applied. A difference grid was subsequently created from the filtered points with the splines in tension algorithm. Adding the difference grid to the GEBCO_2014 grid adjusted the predicted bathymetry grid to the sounding data of the DBM-BATDRAKE database. Artefacts in the transition zone between sounding data and predicted bathymetry were smoothed with the bending algorithm using a transition zone of a 10 km distance buffer around sounding data of the DBM-BATDRAKE database. In the transition zone, the influence of the adjusted predicted bathymetry depth values increased with increasing distance to sounding data. Grid cells directly constrained by sounding data and adjusted predicted bathymetry outside the transition zone remained unchanged. This method successfully prevented unrealistic discontinuities in the seafloor shape, caused by the higher resolving ability of direct measurements compared to predicted bathymetry while integrating the predicted bathymetry smoothly into the resulting surface where data gaps exist.

2.4. Magnetic lineations and seismicity

Additional useful geological information have been included in the map as magnetic lineations, seismicity and main tectonic regimes (Figure 3(B) and Main Map). The seafloor magnetic lineations and theirs magnetic chrons (age attribution) have been compiled from various sources (Eagles & Jokat, 2014; Geletti, Lodolo, Schreider, & Polonia, 2005; Ghidella et al., 2011; Jabaloy et al., 2003; Livermore et al., 2000, 2004; Maldonado et al., 2000, 2014; Scotia Arc Map, 1985) and the position and orientation have been rectified taking into account the detailed image of the tectonic fabric of the oceanic crust. The magnetic timescale is based in Cande & Kent, 1995. The historical seismicity epicentres have been plotted classified by depth and magnitude. The database used is the USGS ANSS Comprehensive Catalog. The relative plate motions vectors used are derived from the TLP2003 model (Thomas, Livermore, & Pollitz, 2003) and they are in agreement with Smalley Jr. et al. (2003, 2007). The main tectonic structures regimes are compiled from regional sources (Barker, 2001; Bohoyo et al., 2007; Eagles & Jokat, 2014; Galindo-Zaldívar et al., 1996; Thomas et al., 2003).

3. Discussion

The bathymetric map based on the DBM-BATDRAKE with a 200 m × 200 m cell resolution shows accurately, and in greater detail than existing regional or global bathymetry databases (Figure 4), an overall view of the Drake Passage seafloor morphology. For the first time it shows clearly the relationships of the main tectonic and morphological features, such as the intersections of the Phoenix–Antarctic and West Scotia ridges with

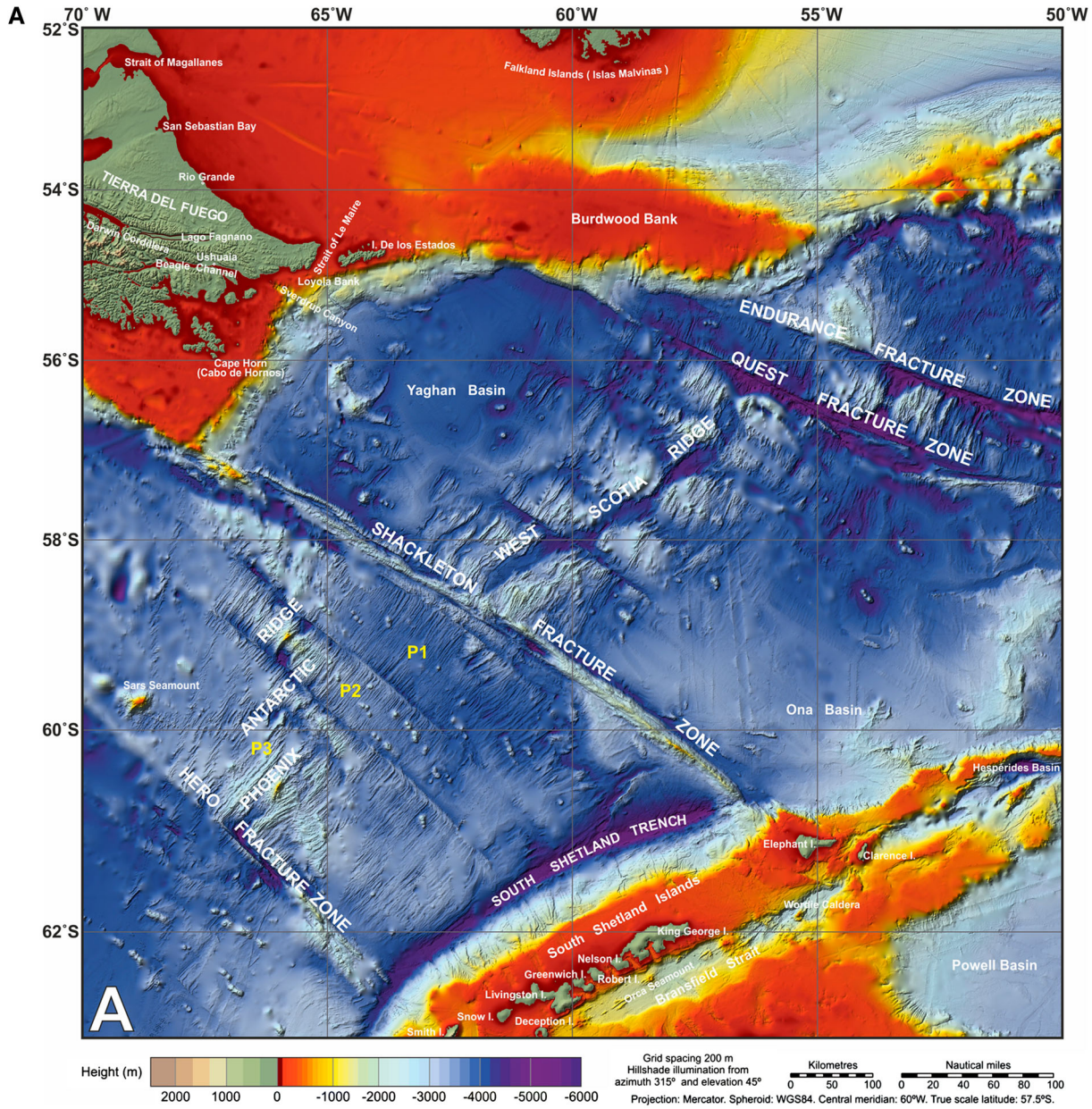

Figure 3. (A) Bathymetry map of the Drake Passage with the colour ramp used in the Main Map and main geographical signatures (B) Bathymetry map in grey ramp including additional geological information as seismicity (depth and magnitude), magnetics (magnetic lineation chrons), tectonics (relationship between plates or major structures and plate motion velocity with Scotia Plate fixed according to Thomas et al., 2003).

the Shackleton Fracture Zone and the connections of the latter to the continental margins of Tierra del Fuego (South America) and the South Shetland Islands block and trench (NE Antarctic Peninsula) (Figure 3 and Main Map). From the bathymetric map is possible to differentiate two main domains: the South America, Antarctic and South Shetland continental margins, including shelf and slope areas, in warm colours (reds, oranges, yellows), and the oceanic domain including the continental rise and ocean basins, in cool colours (blues and purples). This differentiation in general correlates with continental crust and oceanic crust areas, respectively, where the –2000 m isobaths mark roughly this boundary. Each domain contains different kinds of morphological structures that have been developed by tectonic and sedimentary (related with bottom currents or glacial activity) processes (Figure 3).

Although the spreading in the Phoenix–Antarctic and West Scotia ridges ended at 2.6 and 6.4 Ma respectively, abyssal hill fabric in central Drake Passage is well-resolved, in part as consequence of continual scouring by the main jet of the ACC. The intermediate segment of the Phoenix–Antarctic Ridge (P2) is characterized by anomalously shallow median valley walls (Figure 3(A)), that on the northern flank rise to a depth of just 550 m (Livermore et al., 2000). The SW segment (P3) is more complex, with the large-scale rotation of abyssal hill fabric (Figure 3(A)). The deep, sediment-filled, median valley of the West Scotia Ridge is flanked by exposed basement, shallowest on

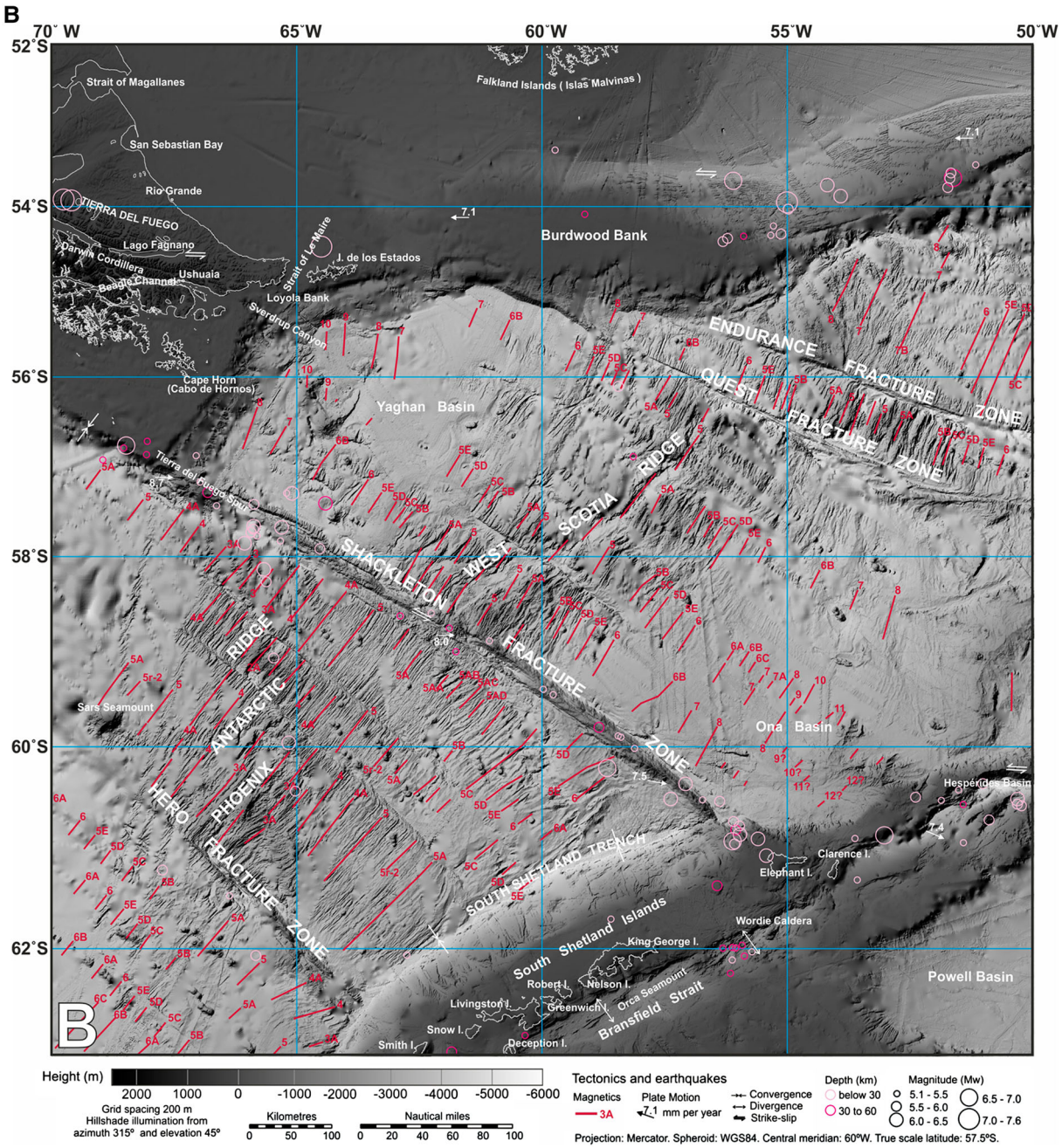

Figure 3 *Continued*

the southern flank. Several long fractures zones are well defined, the Endurance and Quest fracture zones showing the largest offsets of the spreading ridge, and more complexity with an E-W inception. Most of the abyssal hill fabric is isolated into separate areas between fracture zones and interrupted by numerous submarine seamounts and volcanoes, of which there are more than 120 in the map area, and is distributed on both sides of the SFZ.

The sedimentary processes in the region are dominated along the margins by deep oceanic currents that have produced erosional features (e.g. around obstacles such as seamounts, exposing the abyssal hill fabric) and depositional features such as different types of sediment drifts (Figure 3 and Main Map). The South Shetlands Trench morphology shows the effects of along-axis currents on trench-fill sediments. On both the southern and northern continental margins, the dominating erosional processes are also characterized by dense networks of canyons, troughs, gullies and scarps, reflecting downslope transport from the shelf to the deep sea. Significant Mass Transport Deposits have been identified in the region (Pérez et al., 2016). The main operating geological processes in the region at the present-day are related to deep oceanic bottom currents, tectonic processes and glacial dynamics.

4. Conclusions

The bathymetry and geological map of Drake Passage are mainly based on a compilation of precise multibeam bathymetric data obtained on more than 120

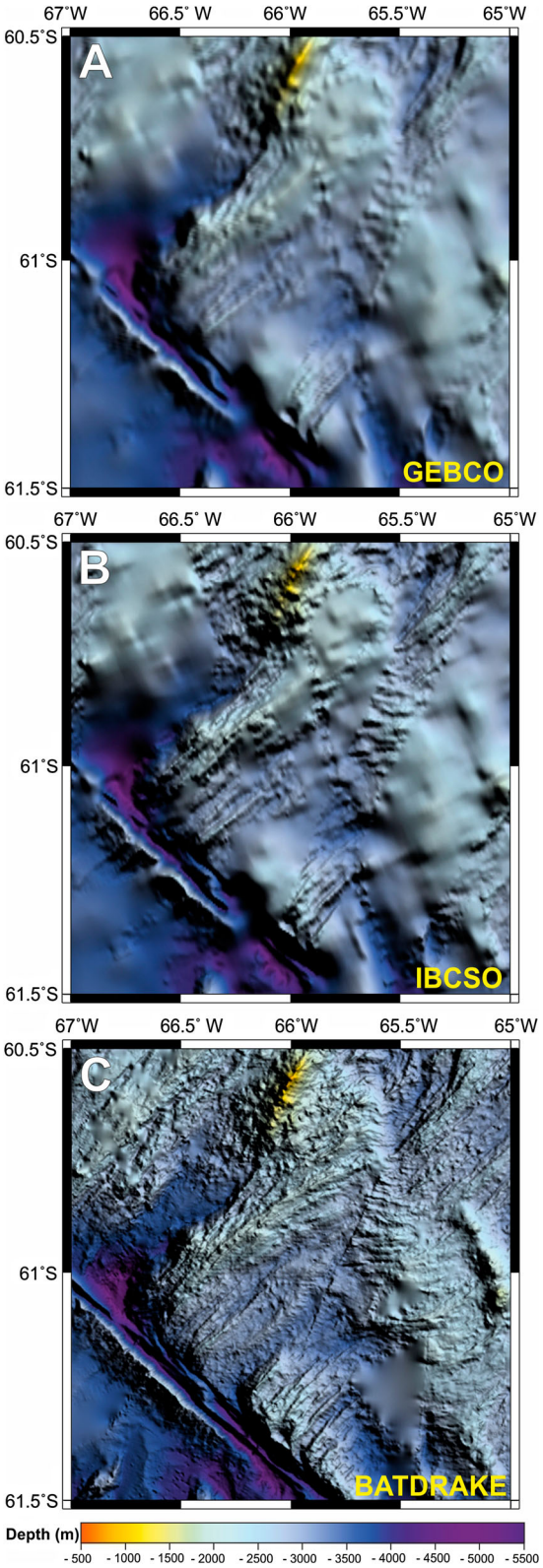

Figure 4. Comparison between available bathymetrical sources in the area around the intersection of the Phoenix–Antarctic Ridge and the Hero Fracture Zone (a) GEBCO_2014 (b) IBCSO v1.0 and (c) DBM-BATDRAKE.

cruises between 1992 and 2015. It covers the area about 1,465,000 km^2 between parallels 52°S and 63°S and meridians 70°W and 50°W. The map, at 1:1,600,000 scale, is projected in Mercator projection using WGS84 ellipsoid. It is based on a new DBM with a 200 m × 200 m cell resolution (DBM-BATDRAKE) displayed as a colour image using a colour table ranging from −6000 to 2500 m (Figure 3 and Main Map). Additional useful geological information includes seafloor magnetic lineations and associated chrons, historical seismicity location classified by depth and magnitude, relative plate motions vectorsand the main tectonic structures regimes (Figure 3 (B)). A brief geological setting description, including the main scientific and cartographic references, is also included (Main Map).

Digital Bathymetric Models are very important in geosciences, physical sciences and life sciences. The seafloor topography in the Drake Passage region is an important boundary condition for high-resolution ocean circulation models and provides constraints on geodynamic models for the initiation and opening of Drake Passage. This new digital bathymetric model (DBM-BATDRAKE) together the bathymetry and geological map of the Drake Passage region represents an important resource to the Antarctic scientific community.

Software

The multibeam data were processed and erroneous sounding and outlier points were removed using dedicated, commercial and free, software as Neptune, Caris, QPS Fledermaus and MB-System. The processed data were exported as ASCII XYZ datasets. The cleaned sounding data were prepared, filtered, merged and gridded using the Generic Mapping Tools (GMT) (Wessel & Smith, 1995), QPS Fledermaus and ArcGIS. Final map and colour palette were developed using GlobalMapper and CorelDraw.

Data

BATDRAKE_JoM_2018.tif is a downloadable geotiff file that contains elevation information in metres with a 200 × 200 m cell spacing in a Mercator projection (datum WGS84) in metres of DBM-BATDRAKE with parameters: scale factor of 1, and true scale latitude at 57.5°S.

Acknowledgements

We thank to the crew and technicians of the RRS James Clark Ross, BIO Hespérides, RV Polarstern, RVIB Nathaniel B. Palmer, and the RV Araon and RV Onnuri for their support and cooperation in obtaining these data under sometimes severe sea conditions. The Scientific Committee on Antarctic Research (SCAR) is acknowledged for providing the framework that allowed this broad international venture. The production of the map was supported by SCAR.

Disclosure statement

No potential conflict of interest was reported by the authors.

Funding

This work was supported through projects CTM2014-60451-C2-02/01, CTM2017-89711-C2-2/1-P and special action CTM2011-13970-E from "Ministerio de Ciencia, Innovación y Universidades" of Spain. This study is part of the British Antarctic Survey Polar Science for Planet Earth Programme funded by the Natural Environment Research Council. This work was also supported by the Scientific Committee on Antarctic Research.

ORCID

F. Bohoyo http://orcid.org/0000-0002-1044-8816
R. D. Larter http://orcid.org/0000-0002-8414-7389
A. J. Tate http://orcid.org/0000-0002-7880-3271
J. E. Arndt http://orcid.org/0000-0002-9413-1612
A. Maestro http://orcid.org/0000-0002-7474-725X
T. R. Riley http://orcid.org/0000-0002-3333-5021

References

Aldaya, F., & Maldonado, A. (1996). Tectonics of the triple junction at the southern end of the Shackleton Fracture Zone (Antarctic Peninsula). *Geo-Marine Letters*, *16*, 279–286.

Arndt, J. E., Schenke, H. W., Jakobsson, M., Nitsche, F. O., Buys, G., Goleby, B., … Wigley, R. (2013). The International Bathymetric Chart of the Southern Ocean (IBCSO) Version 1.0. A new bathymetric compilation covering circum-Antarctic waters. *Geophysical Research Letters*, *40*, 3111–3117.

Barker, P. F. (2001). Scotia Sea regional tectonic evolution: Implications for mantle flow and palaeocirculation. *Earth-Science Reviews*, *55*, 1–39.

Barker, P. F., & Burrell, J. (1977). The opening of the Drake Passage. *Marine Geology*, *25*, 15–34.

Barker, P. F., Dalziel, I. W. D., & Storey, B. C. (1991). Tectonic development of the Scotia arc region. In R. J. Tingey (Ed.), *The Geology of Antarctica* (pp. 215–248). Oxford: Clarendon Press.

Becker, J. J., Sandwell, D. T., Smith, W. H. F., Braud, J., Binder, B., Depner, J., ... Weatherall, P. (2009). Global bathymetry and elevation data at 30 arc seconds resolution: SRTM30_PLUS. *Marine Geodesy*, *32*(4), 355–371. doi:10.1080/01490410903297766

Bohoyo, F., Galindo-Zaldívar, J., Jabaloy, A., Maldonado, A., Rodríguez-Fernández, J., Schreider, A., & Suriñach, E. (2007). Extensional deformation and development of deep basins associated with the sinistral transcurrent fault zone of the Scotia–Antarctic plate boundary. In W. D. Cunningham & P. Mann (Eds.), *Tectonics of strike-slip restraining and releasing bends* (pp. 203–217). London: Geological Society of London, Special Publication. doi:10.1144/sp290.6

Bohoyo, F., Larter, R. D., Galindo-Zaldívar, J., Leat, P. T., Maldonado, A., Tate, A. J., … Nitsche, F. O. (2016). *Bathymetry and geological setting of the drake passage (1:1.500.000).* BAS GEOMAP 2 Series, Sheet 7, British Antarctic Survey, Cambridge, UK.

Cande, S. C., & Kent, D. V. (1995). Revised calibration of the geomagnetic polarity timescale for the Late Cretaceous and Cenozoic. *Journal of Geophysical Research*, *100*(B4), 6093–6095.

Eagles, G., Gohl, K., & Larter, R. D. (2009). Animated tectonic reconstruction of the Southern Pacific and alkaline volcanism at its convergent margins since Eocene times. *Tectonophysics*, *464*, 21–29. doi:10.1016/j.tecto.2007.10.005

Eagles, G., & Jokat, W. (2014). Tectonic reconstructions for paleobathymetry in Drake Passage. *Tectonophysics*, *611*, 28–50.

Eagles, G., Livermore, R. A., Fairhead, J. D., & Morris, P. (2005). Tectonic evolution of the west Scotia Sea. *Journal of Geophysical Research*, *110*, B02401. doi:10.1029/2004JB003154

Galindo-Zaldívar, J., Bohoyo, F., Maldonado, A., Schreider, A. A., Suriñach, E., & Vazquez, J. T. (2006). Propagating rift during the opening of a small oceanic basin: The Protector Basin (Scotia Arc, Antarctica). *Earth and Planetary Science Letters*, *241*, 398–412.

Galindo-Zaldívar, J., Jabaloy, A., Maldonado, A., & Sanz de Galdeano, C. (1996). Continental fragmentation along the South Scotia Ridge transcurrent plate boundary (NE Antarctic Peninsula). *Tectonophysics*, *242*, 275–301.

Geletti, R., Lodolo, E., Schreider, A. A., & Polonia, A. (2005). Seismic structure and tectonics of the Shackleton Fracture Zone (Drake Passage, Scotia Sea). *Marine Geophysical Researches*, *26*, 17–28.

Ghidella, M. E., Forsberg, R., Greenbaum, J. S., Olesen, A. V., Zakrajsek, A. F., & Blankenship, D. D. (2011). Magnetic anomaly data from a regional survey: From Tierra del Fuego to northern Palmer Land, Antarctic Peninsula. *Latinmag Letters*, *1*(Special Issue A19), 1–7.

González-Casado, J. M., Giner-Robles, J. L., & López-Martínez, J. (2000). Bransfield Basin, Antarctic Peninsula: Not a normal back-arc basin. *Geology*, *28*, 1043–1046.

Hell, B., & Jakobsson, M. (2011). Gridding heterogeneous bathymetric data sets with stacked continuous curvature splines in tension. *Marine Geophysical Researches*, *32*(4), 493–501. doi:10.1007/s11001-011-9141-1

Jabaloy, A., Balanyá, J. C., Barnolas, A., Galindo-Zaldı´var, J., Hernández-Molina, F. J., Maldonado, A., … Vázquez, J. T. (2003). The transition from an active to a passive margin (SW end of the South Shetland Trench, Antarctic Peninsula). *Tectonophysics*, *366*(1–2), 55–81. doi:10.1016/S0040-1951(03)00060-X

Jakobsson, M., L. Mayer, B. Coakley, J. A. Dowdeswell, S. Forbes, B. Fridman, … P. Weatherall. (2012). The International Bathymetric Chart of the Arctic Ocean (IBCAO) Version 3.0. *Geophysical Research Letters*, *39* (12), L12609. doi:10.1029/2012GL052219

Kennett, J. P. (1977). Cenozoic evolution of Antarctic glaciation, the Circum-Antarctic Ocean, and their impact on global paleoceanography. *Journal of Geophysical Research*, *82*, 3843–3860.

Larter, R. D., & Barker, P. F. (1991). Effects of ridge crest-trench interaction on Antarctic–Phoenix spreading: Forces on a young subducting plate. *Journal of Geophysical Research*, *96*(B12), 19586–19607.

Lawver, L. A., & Gahagan, L. M. (2003). Evolution of Cenozoic seaways in the circum-Antarctic region. *Palaeogeography, Palaeoclimatology, Palaeoecology*, *198* (1–2), 11–37. doi:10.1016/S0031-0182(03)00392-4

Lawver, L. A., Gahagan, L. M., & Dalziel, I. W. D. (2011). A different look at Gatewys: Drake Passage and Australia/Antarctica. In J. B. Anderson & J. S. Wellner (Eds.), *Tectonic, climatic, and cryospheric evolution of the Antarctic Peninsula.* Washington, DC: AGU-Spec. Pub.63. doi:10.1029/SP063

Livermore, R. A., McAdoo, D., & Marks, K. (1994). Scotia sea tectonics from high resolution satellite gravity. *Earth and Planetary Science Letters*, *150*, 261–275.

Livermore, R. A., Balanyá, J. C., Maldonado, A., Martínez, J. M., Rodríguez-Fernández, J., Sanz de Galdeano, C., … Viseras, J. (2000). Autopsy on a dead spreading centre: The Phoenix Ridge, Drake Passage, Antarctica. *Geology*, 28: 607–610.

Livermore, R., Eagles, G., Morris, P., & Maldonado, A. (2004). Shackleton fracture zone: No barrier to early circumpolar ocean circulation. *Geology*, *32*(9), 797–800.

Livermore, R., Nankivell, A., Eagles, G., & Morris, P. (2005). Paleogene opening of Drake Passage. *Earth and Planetary Science Letters*, *236*(1–2), 459–470.

Livermore, R., Hillenbrand, C-D, Meredith, M., & Eagles, G. (2007). Drake Passage and Cenozoic climate: An open and shut case? *Geochemistry, Geophysics, Geosystems*, *8*, Q01005. doi:10.1029/2005GC001224

Maestro, A., López-Martínez, J., Galindo-Zaldívar, J., Bohoyo, F., & Mink, S. (2014). Evolution of the stress field in the southern Scotia Arc from the late Mesozoic to the present-day. *Global and Planetary Change*, *123*, 269–297.

Maldonado, A., Balanyá, J. C., Barnolas, A., Galindo-Zaldivar, J., Hernández, J., Jabaloy, A., … Viseras, C. (2000). Tectonics of an extinct ridge-transform intersection, Drake Passage (Antarctica). *Marine Geophysical Researches*, *21*(1-2), 43–67.

Maldonado, A., Bohoyo, F., Galindo-Zaldívar, J., Hernández-Molina, F. J., Lobo, F. J., Lodolo, E., … Somoza, L. (2014). A model of oceanic development by ridge jumping: Opening of the Scotia Sea. *Global and Planetary Change*, 123, 152–173. doi:10.1016/j.gloplacha.2014.06.010

Maldonado, A., Larter, R. D., & Aldaya, F. (1994). Forearc tectonic evolution of the South Sheltand margin, Antarctic Peninsula. *Tectonics*, *13*(6), 1345–1370.

Martos, Y. M., Galindo-Zaldívar, J., Catalán, M., Bohoyo, F., & Maldonado, A. (2014). Asthenospheric Pacific-Atlantic flow barriers and the West Scotia Ridge extinction. *Geophysical Research Letters*, *41*, 43–49. doi:10.1002/2013GL058885

Naveira-Garabato, A. C., Heywood, K. J., & Stevens, D. P. (2002). Modification and pathways of Southern Ocean Deep Waters in the Scotia Sea. *Deep-Sea Res. Part I*, *49* (4), 681–705. doi:10.1016/S0967-0637(01)00071-1

Pearce, J. A., Leat, P. T., Barker, P. F., & Millar, I. L. (2001). Geochemical tracing of Pacific-to-Atlantic upper-mantle flow through the Drake Passage. *Nature*, *410*(6827), 457–461. doi:10.1038/35068542

Pérez, L. F., Bohoyo, F., Hernández-Molina, F. J., Casas, D., Galindo-Zaldívar, J., Ruano, P., & Maldonado, A. (2016). Tectonic activity evolution of the Scotia-Antarctic Plate boundary from mass transport deposit analysis. *Journal of Geophysical Research Solid Earth*, *121*. doi:10.1002/2015JB012622

Roterman, C. N., Copley, J. T., Linse, K. T., Tyler, P. A., & Rogers, A. D. (2013). The biogeography of the yeti crabs (Kiwaidae) with notes on the phylogeny of the Chirostyloidea (Decapoda: Anomura). *Proceedings of the Royal Society B*, *280*, 20130718. doi:10.1098/rspb.2013.0718

Scher, H. D., & Martin, E. E. (2006). Timing and climatic consequences of the opening of Drake Passage. *Science*, *312*(5772), 428–430. doi:10.1126/science.1120044

Scher, H. D., Whittaker, J. M., Williams, S. E., Latimer, J. C., Kordesch, W. E., & Delaney, M. L. (2015). Onset of Antarctic Circumpolar Current 30 million years ago as Tasmanian Gateway aligned with westerlies. *Nature*, *523* (7562), 580–583. doi:10.1038/nature14598

Schöne, T., & Schenke, H. W. (1998). Gravity field determination in ice covered regions by altimetry. In R. Forsberg, M. Feissel, & R. Dietrich (Eds.), *Geodesy on the Move, IAG Symp. Proc., 119* (pp. 159–162). Berlin: Springer.

Sievers, H. A., & Nowlin Jr., W. D. (1984). The stratification and water masses at Drake Passage. *Journal of Geophysical Research*, *89*(C6), 10489–10514. doi:10.1029/JC089iC06p10489

Smalley Jr., R., Kendrick, E., Bevis, M. G., Dalziel, I. W. D., Taylor, F., Lauría, E., … Piana, E. (2003). Geodetic determination of relative plate motion and crustal deformation across the Scotia-South America plate boundary in eastern Tierra del Fuego. *Geochemistry, Geophysics, Geosystems*, *4* (9), 1070. doi:10.1029/2002GC000446

Smalley Jr., R., Dalziel, I. W. D., Bevis, M. G., Kendrick, E., Stamps, D. S., King, E. C., … Parra, H. (2007). Scotia arc kinematics from GPS geodesy. *Geophysical Research Letters*, *34*, L21308. doi:10.1029/2007GL031699

Smith, W. H. F., & Sandwell, D. T. (1997). Global seafloor topography from satellite altimetry and ship depth soundings. *Science*, *277*, 1957–1962.

Tectonic Map of the Scotia Arc. 1:3 000 000. BAS (Misc.) 3. British Antarctic Survey Cambridge.

Thomas, C., Livermore, R., & Pollitz, F. (2003). Motion of the Scotia Sea plates. *Geophysical Journal International*, *155*, 789–804.

USGS ANSS Comprehensive Catalog (ComCat). Retrieved from http://earthquake.usgs.gov/

Weatherall, P., Marks, K. M., Jakobsson, M., Schmitt, T., Tani, S., Arndt, J. E., … Wigley, R. (2015). A new digital bathymetric model of the world's oceans. *Earth and Space Science*, *2*, 331–345. doi:10.1002/2015EA000107

Wessel, P., & Smith, W. H. F. (1995). New version of the generic mapping tools released. *Eos, Transactions American Geophysical Union*, *76*, 329.